



HAL
open science

Changes in Phase Behavior from the Substitution of Ethylene Oxide with Carbon Dioxide in the Head Group of Nonionic Surfactants

Vivian J Spiering, Aurora Ciapetti, Michelle Tupinamba Lima, Dominic W Hayward, Laurence Noirez, Marie-sousai Appavou, Reinhard Schomäcker, Michael Gradzielski

► **To cite this version:**

Vivian J Spiering, Aurora Ciapetti, Michelle Tupinamba Lima, Dominic W Hayward, Laurence Noirez, et al.. Changes in Phase Behavior from the Substitution of Ethylene Oxide with Carbon Dioxide in the Head Group of Nonionic Surfactants. *ChemSusChem*, 2020, 13, pp.601 - 607. 10.1002/cssc.201902855 . hal-03028492

HAL Id: hal-03028492

<https://hal.science/hal-03028492v1>

Submitted on 27 Nov 2020

HAL is a multi-disciplinary open access archive for the deposit and dissemination of scientific research documents, whether they are published or not. The documents may come from teaching and research institutions in France or abroad, or from public or private research centers.

L'archive ouverte pluridisciplinaire **HAL**, est destinée au dépôt et à la diffusion de documents scientifiques de niveau recherche, publiés ou non, émanant des établissements d'enseignement et de recherche français ou étrangers, des laboratoires publics ou privés.

Changes in Phase Behavior from the Substitution of Ethylene Oxide with Carbon Dioxide in the Head Group of Nonionic Surfactants

Vivian J. Spiering,^{*,[a]} Aurora Ciapetti,^[a] Michelle Tupinamba Lima,^[b] Dominic W. Hayward,^[a] Laurence Noirez,^[c] Marie-Sousai Appavou,^[d] Reinhard Schomäcker,^[b] and Michael Gradzielski^{*,[a]}

Nonionic ethylene oxide (EO)-based surfactants are widely employed in commercial applications and normally form gel-like liquid crystalline phases at higher concentrations, rendering their handling under such conditions difficult. By incorporating CO₂ units in their hydrophilic head groups, the consumption of the petrochemical EO was reduced, and the tendency to form liquid crystals was suppressed completely. This surprising behavior was characterized by rheology and studied with respect to its structural origin by means of small-angle neutron scattering (SANS). These experiments showed a strongly reduced re-

pulsive interaction between the micellar aggregates, attributed to a reduced hydration and enhanced interpenetration of the head groups owing to the presence of the CO₂ units. In addition, with increasing CO₂ content the surfactants became more efficient and effective with respect to their surface activity. These findings are important because the renewable resource CO₂ is used, and the CO₂-containing surfactants allow handling at very high concentrations, an aspect of enormous practical importance.

Introduction

Nonionic surfactants with ethylene oxide [EO; or ethylene glycol (EG)] head groups are the workhorse surfactants in the field of detergency and many other applications of surfactants.^[1,2] For example, in the European Union, more than 1 mil-

lion tons are produced per year.^[3] EO is a petrochemical product, and for such a large-scale product it is interesting to substitute it by biorenewable resources. One option that has been explored so far in that direction is the use of glycerol for the head group,^[4] and with such surfactants also nanoemulsions can be formed.^[5] However, in the field of detergency they have not been able to substitute conventional nonionic surfactants, and here researchers are still searching for a more sustainable chemical solution.

In our experiments, we studied nonionic surfactants that were modified in terms of their head group, containing different numbers of CO₂ moieties that partly substitute the EO units. The use of CO₂ as a resource in organic chemistry and also, in particular, its copolymerization with epoxides is a topic of high current interest. The process itself has been known for over 40 years but has seen substantial catalytic improvements in recent years.^[6–9] Application of such synthetic schemes, for instance, led to the formation of nanostructures from CO₂-based polycarbonates^[10] or functional copolymers based on CO₂ and glycidyl ethers.^[11]


In our case, CO₂-modified surfactants were obtained by a double metal cyanide (DMC)-catalyzed copolymerization of a mixture of EO and CO₂ with a monofunctional alkanol as starting unit^[12,13] (here: dodecanol). By doing so and varying the relative amount of CO₂, nonionic surfactants with different CO₂ content in their head group are accessible (Figure 1), which apart from this are identical with respect to their hydrophobic group and the length of their hydrophilic head (see Table S1 in the Supporting Information). Such surfactants are of high inter-


[a] V. J. Spiering, A. Ciapetti, Dr. D. W. Hayward, Prof. Dr. M. Gradzielski
Stranski-Laborator für Physikalische und Theoretische Chemie
Institut für Chemie
Technische Universität Berlin
Straße des 17. Juni 124, 10623 Berlin (Germany)
E-mail: v.spiering@tu-berlin.de
michael.gradzielski@tu-berlin.de

[b] M. T. Lima, Prof. Dr. R. Schomäcker
Institut für Chemie—Technische Chemie
Technische Universität Berlin
Straße des 17. Juni 124, 10623 Berlin (Germany)

[c] Dr. L. Noirez
Laboratoire Léon Brillouin (CEA-CNRS)
C.E.-Saclay, 91191 Gif sur Yvette Cedex (France)

[d] Dr. M.-S. Appavou
Forschungszentrum Jülich GmbH
Jülich Centre for Neutron Science (JCNS) at Heinz Maier-Leibnitz Zentrum (MLZ)
Lichtenbergerstr. 1, 85747 Garching (Germany)

 Supporting Information and the ORCID identification number(s) for the author(s) of this article can be found under:
<https://doi.org/10.1002/cssc.201902855>.

 © 2019 The Authors. Published by Wiley-VCH Verlag GmbH & Co. KGaA. This is an open access article under the terms of the Creative Commons Attribution Non-Commercial NoDerivs License, which permits use and distribution in any medium, provided the original work is properly cited, the use is non-commercial, and no modifications or adaptations are made.

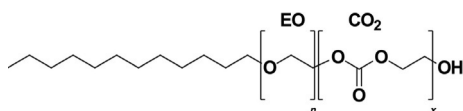


Figure 1. General structural formula of the CO₂-containing nonionic dodecyl surfactants investigated in this work; in particular we studied: C₁₂EO_{14.0}-OH, C₁₂(CO₂)_{0.6}EO_{13.3}-OH, C₁₂(CO₂)_{1.3}EO_{11.4}-OH, C₁₂(CO₂)_{1.5}EO_{11.6}-OH, and C₁₂(CO₂)_{3.1}EO_{8.2}-OH.

est because of the substitution of the petrochemical EO unit by CO₂ as a cheap and environmentally benign resource. In addition, the CO₂ units are diesters, which typically can be degraded more easily (a point of ecological importance).

Owing to their high importance, the properties of nonionic surfactants have been studied in detail. Key features are their self-assembly behavior in aqueous solution, which shows a marked temperature dependence, and at higher concentrations, they form liquid crystalline (LC) phases.^[1,14] The type and location of these LC phases in the phase diagram depends in a systematic fashion on the molecular architecture of the nonionic EO surfactants.^[14,15] Typically, hexagonal and cubic phases are formed, which exhibit marked gel-like properties (with shear moduli G_0 in the range of 10⁴–10⁶ Pa).^[16,17] This behavior is often problematic because for many formulations the formation of highly viscous phases during the preparation process is a major nuisance and therefore has to be avoided or circumvented. This often means one has to work in application/formulation with accordingly diluted surfactants from the very beginning, which leads to substantially higher logistic costs and volumes, thereby having a negative ecological impact.

In our work, we were now interested in how CO₂-containing surfactants compare to their conventional nonionic counterparts. Accordingly, we studied a series of dodecyl surfactants in which the amount of contained CO₂ units was systematically varied [i.e., C₁₂(CO₂)_xEO_n with x in the range of 0–3.1 and $n = 8.2$ –14.0; see Figure 1 and Table S1 in the Supporting Information]. Here it should be noted that the distribution of the CO₂ in the head group is statistical (see Figure S1 in the Supporting Information). The synthesis and basic properties have been described before,^[13] including their hydrophilic–lipophilic balance and behavior in the formation of emulsions, which showed a similar property spectrum as their conventional analogues.^[18]

Results and Discussion

Phase behavior and surface activity

A key property in the characterization of new surfactants is their surface activity, and it allows to determine the critical micelle concentration (cmc). The surface tension data of all four CO₂-containing surfactants look quite similar (Figure 2), with a cmc value of 0.053 mmol L⁻¹ for the surfactant with the highest CO₂ content [C₁₂(CO₂)_{3.1}EO_{8.2}-OH] and 0.175 mmol L⁻¹ for the surfactant without CO₂ (C₁₂EO_{14.0}-OH). Surface tension measurement data for the individual surfactants are shown in Figure S2 in the Supporting Information. From this change in cmc values, one may conclude that the surfactants become more

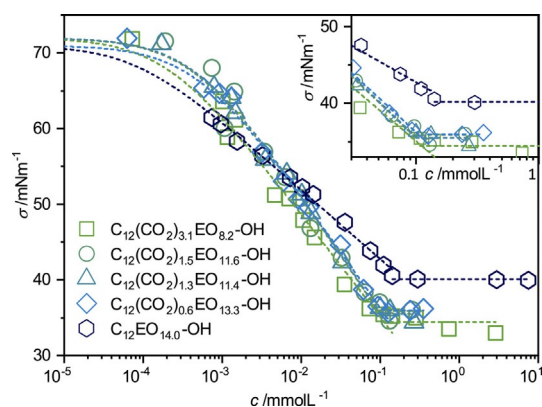


Figure 2. Surface tension σ as a function of concentration for C₁₂EO_{8.2}(CO₂)_{3.1}-OH, C₁₂EO_{11.6}(CO₂)_{1.5}-OH, C₁₂EO₁₄(CO₂)_{1.3}-OH, C₁₂EO_{13.3}(CO₂)_{0.6}-OH, and the reference sample C₁₂EO_{14.0}-OH at 25 °C.

hydrophobic with increasing CO₂ content (Figure S3, left in the Supporting Information). The obtained values are lower compared with other nonionic C₁₂ surfactants at 25 °C, such as *n*-dodecyl- β -D-glucoside with 0.19 mmol L⁻¹^[19] or C₁₂EO₅-OH with 0.064 mmol L⁻¹,^[20] thereby indicating a higher extent of hydrophobicity. The cmc, the head group areas (a_0), and the Gibbs free energy of micellization (ΔG_{mic}) of the different surfactants are summarized in Table 1. The surface tension of the CO₂ surfactants at 25 °C at the cmc was found to be between 34.4 and up to 35.9 mN m⁻¹. This is in the expected range for C₁₂EO_j nonionic surfactants,^[21–23] but it is interesting to note that surface tension becomes lower with increasing CO₂ content, that is, the surfactants become more effective.

Table 1. Summary of the surface tension measurements.^[a]

Surfactant	cmc [mmol L ⁻¹]	σ_{CMC} [mN m ⁻¹]	a_0 [nm ²]	ΔG_{mic} [kJ mol ⁻¹]
C ₁₂ (CO ₂) _{3.1} EO _{8.2} -OH	0.053	34.4	0.55	–34.3
C ₁₂ (CO ₂) _{1.5} EO _{11.6} -OH	0.091	35.9	0.65	–33.0
C ₁₂ (CO ₂) _{1.3} EO _{11.4} -OH	0.099	35.5	0.67	–32.8
C ₁₂ (CO ₂) _{0.6} EO _{13.3} -OH	0.118	35.9	0.69	–32.4
C ₁₂ EO _{14.0} -OH	0.175	40.1	1.07	–31.4

[a] Critical micelle concentration (cmc), surface tension at the cmc (σ_{CMC}), head group area (a_0), and Gibbs free energy of micellization (ΔG_{mic}).

Furthermore, it was observed that the head group area decreases with increasing CO₂ content (Figure S3 in the Supporting Information). This decrease can be explained by an enhanced hydrophobicity and a decreased hydration. ΔG_{mic} was found to be linearly proportional to the CO₂ content. Performing a linear regression fit to the gradient (Figure S3, right in the Supporting Information) reveals a transfer energy of (–0.37 ± 0.06) kT per CO₂ unit, independent of temperature. This value is substantially smaller than the transfer energy of a CH₂ group in a hydrophobic chain (\approx –1.2 kT), but nonetheless large enough to significantly influence the micellization process. It was previously found that the introduction of hydrophobic propylene oxide (PO) units into the hydrophilic chain of C₁₂EO₈

surfactants gives rise to a transfer energy of -0.25 kT/PO unit at 25 °C.^[24] The effect of adding PO and CO₂ units is therefore similar, in both cases facilitating the formation of micelles, but more pronounced for the case of CO₂ incorporation. For a comparison, the transfer energy per EO unit is $+0.16$ kT,^[25] and thus the EO unit is causing a small contribution disfavoring micellization.

In summary, the CO₂-containing surfactants are having a lower cmc, which means for many applications that one can reduce the required amount, and they also show lower surface tension values above the cmc, as typically wished for a surfactant. Accordingly, substitution of EO by CO₂ in the head group leads to more efficient and effective nonionic surfactants.

Rheological behavior

Most interesting is the behavior at high concentrations as for conventional nonionic surfactants of this type (e.g., C₁₂EO₈^[14] or C₁₂EO₁₂^[26]) one observes with increasing concentration above approximately 25–30 wt% first a cubic phase and at still higher concentration a hexagonal phase is formed, both of which are highly viscous and gel-like in appearance. In contrast, the CO₂-containing nonionic surfactants show a very different phase behavior depicted in Figure 3. For surfactants containing more than one CO₂ unit per molecule in their hydrophilic head group, LC phases are no longer formed. The assignment of the different LC phases was done based on polarization microscopy (the cubic phase is isotropic, whereas the hexagonal phase shows typical fan-like birefringence textures, see Figure S4 in the Supporting Information) and was corroborated by the small-angle neutron scattering (SANS) results (see Figure S5 in the Supporting Information).

The absence of the LC phases for higher CO₂ content is not only interesting for fundamental soft matter science but is also largely altering the flow behavior of such systems, and thereby the way they can be handled in terms of application. The CO₂-containing surfactants with more than one CO₂ unit per molecule are always rather low-viscosity Newtonian fluids ($\eta < 1$ Pa s), whereas conventional nonionic surfactants form

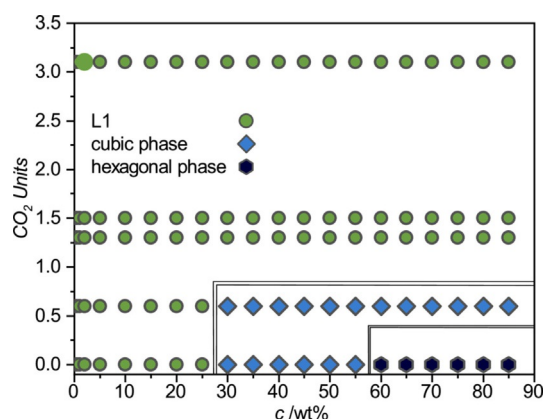


Figure 3. Phase diagram at 25 °C as a function of the surfactant concentration and the number of CO₂ units contained in the hydrophilic head group (with isotropic L₁-phase, cubic phase, and hexagonal phase).

highly viscous gels with a yield stress. This effect of largely changed flow behavior is quantified by the viscosity curves shown in Figure 4a, which directly compare the surfactant without CO₂ and the one containing 3.1 CO₂ units

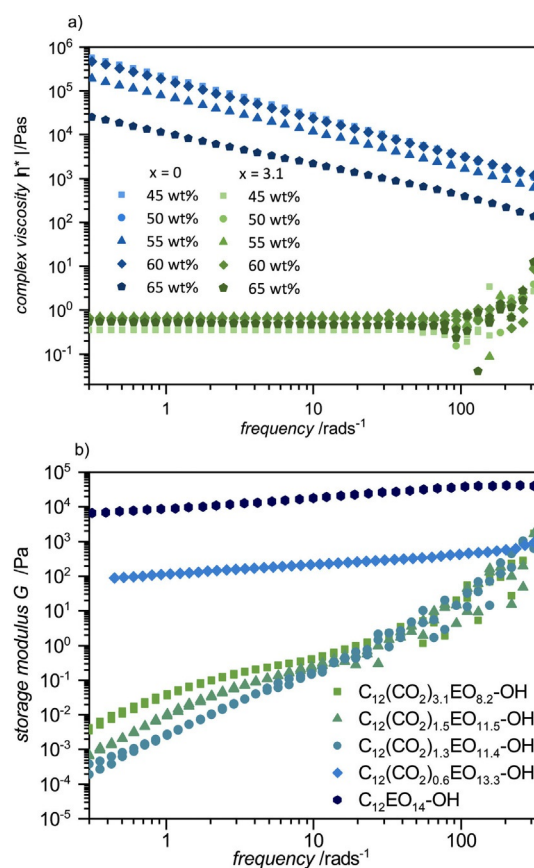


Figure 4. Rheological parameters for different surfactant samples in the high-concentration regime of 45–65 wt% obtained at 25 °C from oscillation measurements at a shear stress of 0.5 Pa. (a) Magnitude of the complex viscosity $|\eta^*|$ as a function of angular frequency for the CO₂-richest surfactant ($x=3.1$) and the reference sample without CO₂ ($x=0$); (b) Storage modulus G' as a function of angular frequency for the different surfactants at constant concentration of 65 wt% (measurement system: cone-plate stainless-steel geometry radius: 40 mm, gap size 150 μ m).

[C₁₂(CO₂)_{3.1}EO_{8.2}-OH] at different concentrations. The latter is in the concentration range from 45 to 65 wt% always a Newtonian liquid with a viscosity of approximately 0.4–0.8 Pa s, whereas for the equivalent conventional surfactant without CO₂ a 4–6 orders of magnitude higher viscosity (no finite zero-shear viscosity is seen, corresponding to having a yield stress) and a reduction with increasing frequency (corresponding to shear thinning) is observed. The storage modulus G' as a function of frequency obtained from oscillatory rheological measurements for the different surfactants at a given concentration of 65 wt% (Figure 4b) shows for C₁₂EO_{14.0}-OH constant values of approximately 2×10^4 Pa s (rather stiff gel; these values depend somewhat on the concentration as shown in Figure S6a in the Supporting Information), which quantifies the gel-like properties of these samples. Already for the surfactant with an average of 0.6 CO₂ units per molecule, the value is reduced by two

orders of magnitude. It is still rather constant, thereby confirming the gel properties, but as a much softer gel. In contrast, for the surfactants containing more than one CO₂ group the values are smaller by four to six orders of magnitude. Actually, the values given in Figure 4b for the samples with $x > 1$ are not really meaningful because the viscous component of the complex shear modulus G^* is largely dominating, as shown in Figure S6b in the Supporting Information.

Small-angle neutron scattering

Apparently, the flow and phase behavior of the concentrated nonionic surfactant solutions are largely changed by the incorporation of the CO₂ moieties into their head groups. To elucidate this interesting phenomenon further, we studied in detail the structure of the self-assembled aggregates formed here and their structural ordering. This was done by SANS experiments, which confirm that at a higher concentration no LC ordering is present, and especially no cubic phases are observed, which typically show pronounced gel-like behavior.^[27] Often cubic phases are manifested in the scattering patterns by spikes on the isotropic correlation peak,^[27–31] as seen for C₁₂EO_{14,0}-OH and C₁₂(CO₂)_{0,6}EO_{13,3}-OH (shown in Figure 5a for samples with 50 wt%; for the scattering patterns at other concentrations see Figure S7 in the Supporting Information). In

contrast, the samples with higher CO₂ content show isotropic scattering rings. When looking more closely at the radially averaged correlation peak at a given concentration of 50 wt% (Figure 5b), one notices that the peaks become increasingly wider and less sharp with increasing CO₂ content. This indicates a much lower degree of ordering, which generally could be attributed to less pronounced repulsive interactions between the micelles. At the same time, the peak position moves somewhat towards smaller q values, which indicates a small micellar growth with increasing CO₂ content in the head group.

SANS measurements at a lower concentration of 1 wt% showed similar scattering curves (Figure S8 in the Supporting Information) that prove that globular micelles of similar size (radius of gyration of 2.4–2.7 nm, Table S3 in the Supporting Information) are always formed, irrespective of the CO₂ content of the surfactant. A quantitative analysis of the SANS data shows that there is some increase in size with increasing content of CO₂ (Table S3 in the Supporting Information), in agreement with the shift of the correlation peak at higher concentration. For spherical micelles, this corresponds to a reduction of the head group area (a_0) from 0.85 nm² for the pure EO surfactant to 0.62 nm² for C₁₂(CO₂)_{3,1}EO_{8,2}-OH (Table S3 in the Supporting Information). These values are in good agreement with the data from surface tension measurements (Table 1). A rational explanation of this observation would be that with increasing CO₂ content a_0 is reduced because of a lower extent of hydration. SANS measurements over a large concentration range up to 65 wt% (see Figure S9 in the Supporting Information) show that the size of the micelles is only slightly affected by the change of concentration (i.e., one has similar aggregates present), but in the case without or with little CO₂ in the head group leading to LC stiff phases, whereas for more than one CO₂ unit in the head groups the fluid state was retained up to highest concentrations. Apparently, the interaction and the extent of ordering at high concentration change largely upon the incorporation of CO₂ into the head groups. To quantify the effective interaction between the micelles as a function of the CO₂ content of the different surfactants, we further analyzed the scattering data in the thermodynamic limit (i.e., $q \rightarrow 0$). The determined $I(0)_{\text{exp}}$ values as a function of the volume fraction ϕ (here considering the “dry” volume fraction ϕ resulting from the surfactant only) are given in Figure 6 and show the expected passing through a maximum at a given ϕ . This can be explained such that the intensity first increases linearly with the number of dispersed particles, but with increasing concentration, they become increasingly ordered (thereby suppressing fluctuations responsible for the scattering). This effect is quantitatively described by the structure factor $S(0)$, which then leads to a reduction in scattering intensity. To describe the experimentally observed scattering behavior, we employed the hard-sphere model according to Carnahan–Starling^[32] [Eq. (1)]:

$$S(0)^{-1} = \frac{(1 + 2\phi_{\text{hs}})^2 - 4\phi_{\text{hs}}^3 + 4\phi_{\text{hs}}^4}{(1 - \phi_{\text{hs}})^4} \quad (1)$$

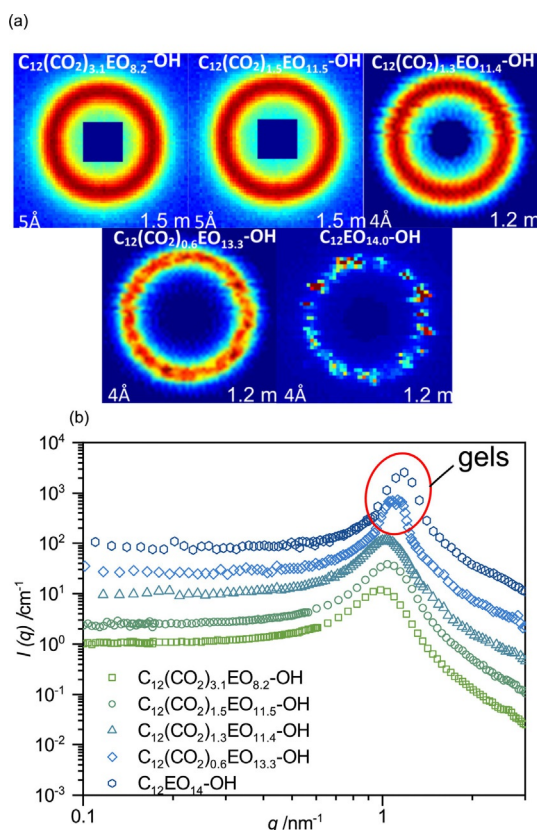


Figure 5. (a) Comparison of 2D scattering patterns of the nonionic surfactants with different CO₂ content in their head groups for a constant concentration of 50 wt%. (b) Radially averaged intensity curves for the same data (indicating the markedly sharper peaks of the gels). The curves are scaled on the y-axis by the following multipliers: (CO₂)_{3,1}:1; (CO₂)_{1,5}:4; (CO₂)_{1,3}:12; (CO₂)_{0,6}:64; (CO₂)₀:240.

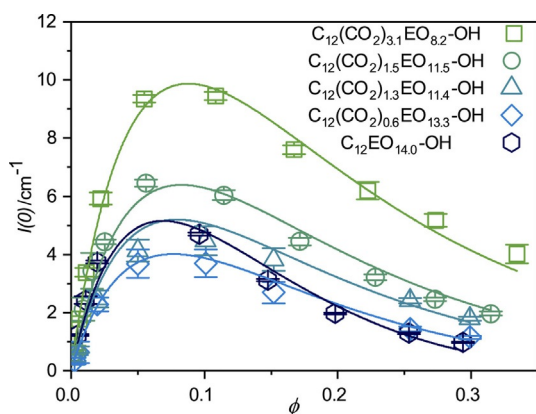


Figure 6. $I(0)_{\text{exp}}$ for all CO_2 surfactants from SANS data depending on the dry volume fraction ϕ . Lines are $I(0)_{\text{th}}$, considering the static structure factor $S(0)$, which was calculated from the volume fraction ϕ_{hs} of the swollen aggregates with a certain amount of water (described by B) and the softness parameter A that describes the extent of interpenetration of the aggregates [Eq. (1)].

in which ϕ_{hs} is the solvated volume fraction effective responsibility for the hard-sphere interaction, and $\phi_{\text{hs}} = B\phi(1 - A\phi)$, in which B quantifies the extent of hydration of the aggregates (i.e., the amount of water strongly bound to the head group) that has to be considered when describing the micelles as hard spheres. A is accounting for the effect of “softness”, which means the extent to which aggregates can interpenetrate at higher concentration, thereby effectively reducing the volume fraction of the system. On this basis, one can calculate directly the observed intensity $I(0)$ according to Equation (2):

$$I(0) = \phi \cdot \Delta(\text{SLD})^2 \cdot V \cdot S(0) \quad (2)$$

which is the monodisperse approximation, in which $\Delta(\text{SLD})$ is the difference of the scattering length densities of (dry) micelles and D_2O , and V the volume of the dry aggregates.

Looking in detail at the experimental data shown in Figure 6 one observes a marked increase in intensity with increasing CO_2 content and at the same time, the relative reduction of intensity beyond the maximum becomes much less pronounced. The higher intensity arises from larger aggregates with increasing CO_2 content, as already seen from the SANS curves taken at 1 wt% (Figure S8 and Table S3 in the Supporting Information). Describing these data with Equations (1) and (2) shows that with increasing CO_2 content there is less hydration of the head groups (smaller B) and therefore a lower effective volume fraction (data summarized in Table 2). The hydration number H of water molecules per surfactant molecule is such that for each EO group one has approximately two water molecules, whereas one can assign nominally zero water molecules per CO_2 group. More importantly, the aggregates become much softer, as evidenced by the substantial increase of A , which means that at higher concentration the effective volume fraction of the aggregates does not increase much. This increase at high concentration is seen even more clearly

Table 2. Parameters from the fits shown in Figure 5 for $I(0)_{\text{exp}}$ from SANS data for volume fractions up to 0.35.^[a]

Surfactant	A	B	H	M_w [kDa]	N_{agg}	a_0 [nm ²]
$\text{C}_{12}(\text{CO}_2)_{3.1}\text{EO}_{8.2}\text{-OH}$	0.55	1.51	17.2	55.4	80.5	0.62
$\text{C}_{12}(\text{CO}_2)_{1.5}\text{EO}_{11.5}\text{-OH}$	0.52	1.58	19.7	35.4	46.4	0.74
$\text{C}_{12}(\text{CO}_2)_{1.3}\text{EO}_{11.4}\text{-OH}$	0.50	1.63	23.2	29.6	39.8	0.86
$\text{C}_{12}(\text{CO}_2)_{0.6}\text{EO}_{13.3}\text{-OH}$	0.37	1.64	25.2	22.8	28.7	0.94
$\text{C}_{12}\text{EO}_{14.0}\text{-OH}$	0.01	1.72	28.8	30.9	38.5	0.85

[a] A , B , hydration number H (molecules of water per surfactant molecule), molecular weight M_w , aggregation number N_{agg} , and head group area a_0 .

ly in Figure S10 in the Supporting Information, in which we normalized the data with respect to the maximum of $I(0)$ and the volume fraction ϕ_{max} at which the maximum is located. This means that the CO_2 -containing micelles are much more interpenetrating (see Figure 7), and thereby much less repulsive and unable to form ordered (LC) phases.

Accordingly, similar micelles are present, but the incorporation of the CO_2 moieties into the hydrophilic head groups leads to a substantial alteration of the interaction potential and renders them much softer. This apparently arises firstly from the lower extent of hydration of the head groups and secondly from attractive interactions owing to the presence of CO_2 units that allow for interpenetration of the hydrophilic corona of the surfactants (see Figure 7). Polyethylene oxide (PEO) is known to be strongly hydrated,^[33,34] but this tendency is reduced by the presence of CO_2 units. Such a reduction of the hydration is concomitant to a reduced a_0 , which in turn explains the formation of larger aggregates based on simple geometry (as the radius of a spherical micelle should be given as $R = 3v_h/a_h$, with v_h being the molecular volume of the hydrophobic part of the surfactant). In addition, it appears that CO_2 units of neighboring micellar head group coronas are less repulsively interacting with each other, presumably because of their strong dipole moment coupled with the high polarizability of the CO_2 group. In summary, the interaction potential between the nonionic micelles becomes much less repulsive, and such “soft spheres” then accordingly do not form highly ordered LC phases with their corresponding gel-like properties (Figure 7).

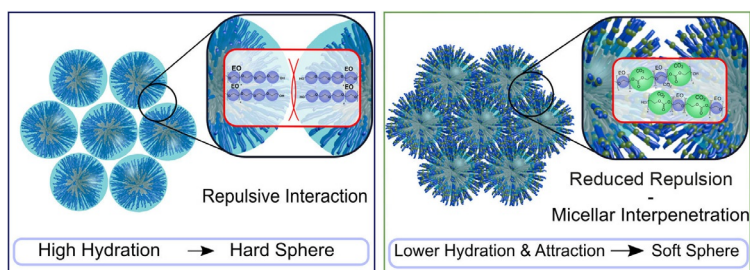


Figure 7. Illustration of the packing conditions prevailing in the case of nonionic surfactants without and with incorporated CO_2 units in the head group. A higher CO_2 content reduces hydration, reducing the repulsive interactions, and thereby allows for interpenetration of the hydrophilic micelles shells.

Conclusions

In this work, we studied the effect of replacing petrol-based ethylene oxide (EO) in the head groups of nonionic surfactants by the renewable resource CO₂. The presence of CO₂ in the head group reduces the critical micellar concentration (cmc) and the surface tension above the cmc (i.e., the surfactants become more efficient and effective). Most interestingly, our study shows that the phase behavior of nonionic surfactants is fundamentally altered by substituting CO₂ moieties into the hydrophilic EO-based head groups. Already the incorporation of one CO₂ group per molecule suppresses the formation of gel-like liquid crystalline phases completely. This is not only fundamentally a very interesting observation but also one of high practical importance, facilitating enormously the handling of these surfactants at higher concentrations, which is typically required in almost all applications at some stage. It should also be noted that this behavior is unique for CO₂ incorporation; for instance, the incorporation of the hydrophobic propylene oxide (PO) unit, even at a much higher percentage of substitution, still leads to the formation of a gel-like phase (e.g., shown for C₁₂EO₄PO₃).^[35]

Scattering experiments show that the origin of this surprising behavior is a substantial dehydration of the head groups owing to the presence of the CO₂ moieties and a considerably reduced repulsive interaction and interpenetration between the head groups. Together, this causes the repulsiveness of the interactions to become too weak to allow a higher ordering of the micelles, and therefore no liquid crystalline phases are formed.

This is an interesting example of how a fundamental investigation of the structural and phase behavior of a surfactant system allows for a systematic understanding based on the molecular architecture. Being able to work at any concentration allows for more compact shipment, thereby reducing substantially the ecological impact of the logistics for this large-scale commodity product. This information can be applied directly in surfactant science for formulation at high concentrations. In addition, these CO₂-containing surfactants contribute to the aim of more sustainable chemistry as the petrol based EO units are replaced by CO₂ (by up to 25%). Furthermore, even less surfactant has to be employed for typical applications because the CO₂ incorporation also reduces the cmc, owing to the fact that the CO₂ groups render the surfactant more hydrophobic; the transfer energy for micellization is changed by -0.37 kT per CO₂ unit. Finally, above the cmc the CO₂-containing surfactants also show lower surface tension values (i.e., they are more effective surfactants). For all these reasons, and with this simple synthetic approach, it can be expected that CO₂-containing nonionic surfactants will become a very promising alternative in the surfactant market.

Experimental Section

Surface tension measurements were performed with a du-Noüy ring on a DCAT tensiometer (Data Physics) at 25, 30, 40, and 50 °C. The temperature was maintained by a circulating thermostat with

prior heating of the surfactant solution in an oven and an equilibration time of 20 min. The surface tension was measured until the value remained constant for a given period, as defined by the measurement software (typically 350 s). The measured average surface tension was determined for each in a concentration range from 10⁻⁵ up to 0.02 wt% and plotted as a function of logarithmic concentration. The cmc was determined by calculating the point at which the surface tension reaches a constant plateau value. In addition, the surface tension measurements were used to determine the surface excess concentration (Γ) and the head group area (a_0) using the Langmuir–Szyszkowski isotherm^[36] [Eq. (3)]:

$$\sigma = \sigma_0 - RT\Gamma \cdot \ln(1 + Kc) \quad (3)$$

in which σ is the surface tension [Nm⁻¹], σ_0 the surface tension of water (72.8 mNm⁻¹ at 298 K), R the ideal gas constant (8.314 JK⁻¹mol⁻¹), T the temperature, Γ the surface excess concentration, K the absorption constant, and c the concentration. The head group area a_0 is related to the surface excess concentration by the Avogadro constant, N_A , by Equation (4):

$$a_0 = (\Gamma \cdot N_A)^{-1} \quad (4)$$

According to the phase-separation model^[37] and the mass-action model^[38] the standard Gibbs free energy of micellization per mole of monomer (ΔG_{mic}) is given by Equation (5):

$$\Delta G_{mic} = RT \cdot \ln \chi_{cmc} \quad (5)$$

in which χ_{cmc} is the mole fraction of surfactant in aqueous solution at the cmc (assuming ideal behavior).

Rheology measurements were performed with a Bohlin Gemini 200 HR nano rheometer (Malvern Instruments), using a cone-plate geometry (radius: 40 mm, gap size 150 μ m, stainless-steel geometry). In steady-state conditions, the applied shear rates varied from 0.0014 to 50 s⁻¹. To analyze the viscoelastic behavior of these samples, oscillatory measurements were performed with the same instrument and fixtures. A strain amplitude sweep was performed at a constant angular frequency of 6.3 Hz varying the amplitude of the shear stress at 0.01–15 Pa to identify the linear viscoelastic regime. Based on these measurements a frequency sweep at a shear stress of 0.5 Pa and angular frequencies varying from 0.6–314.2 Hz was performed to determine the storage modulus G' and the loss modulus G'' . The reference surfactant was analysed with a MCR301 rheometer (Anton Paar) under the same measurement conditions.

SANS was measured at the Heinz Maier-Leibnitz Zentrum (MLZ) in Munich, Germany, on the Instrument KWS-1^[39] and at the Laboratoire Léon Brillouin (LLB) in Saclay, France, on the instrument PAXY. KWS-1 was operated at a wavelength of 5 Å and a sample-to-detector distances (SDD) of 1.5 to 20 m, to cover a q -range of 0.015–4 nm⁻¹. Sample transmissions were measured at a SDD of 8 m. For all scattering data, the intensities were divided by the corresponding transmission and sample thickness (1 mm), corrected for the empty cell, and normalized with respect to the scattering of a 1 mm sample of light water, according to standard procedures.^[40] The incoherent background was determined by a Porod plot. The SANS measurements performed at PAXY were performed at a wavelength of 4 Å for SDDs of 1.2 and 5 m, and a wavelength of 12 Å for an SDD of 6 m, thereby covering a q -range of 0.02–6 nm⁻¹.

Acknowledgements

This work has been carried out within the project “Dream Resource” (033RC002C). The project is funded by the German Federal Ministry of Education and Research (BMBF) within the funding priority “CO₂ Plus—Stoffliche Nutzung von CO₂ zur Verbesserung der Rohstoffbasis”. Covestro Deutschland AG is much thanked for providing the surfactants and M. Sebastian and M. Weinkraut for input regarding this manuscript. In addition, we are grateful to the LLB and JCNS for allocating SANS beam times. This work is based upon experiments performed at the KWS-1 instrument operated by JCNS at the Heinz Maier-Leibnitz Zentrum (MLZ), Garching, Germany and at the PAXY instrument at the Laboratoire Léon Brillouin (LLB, CEA-CNRS). Additionally, we would like to thank Professor Auhl for the use of the MCR301 Rheometer.

Conflict of interest

The authors declare no conflict of interest.

Keywords: carbon dioxide · liquid crystals · low viscosity · nonionic surfactants · small-angle neutron scattering

- [1] *Nonionic Surfactants: Physical Chemistry* (Ed.: M. J. Schick), Marcel Dekker, New York, **1987**.
- [2] *Industrial Application of Surfactants IV, Vol. 4* (Ed.: D. R. Karsa), Royal Society of Chemistry, London, **1999**.
- [3] H. Janshekar, E. Greiner, T. Kumamoto, Y. (Eva) Zhang, *Surfactants - Specialty Chemicals Update Program (SCUP)*, IHS Chemicals, **2015**, <https://ihsmarkit.com/products/chemical-surfactants-scup.html>.
- [4] H. Wenk, J. Meyer, *SOFW J.* **2009**, *135*, 25–30.
- [5] P. Heunemann, S. Prévost, I. Grillo, C. M. Marino, J. Meyer, M. Gradzielski, *Soft Matter* **2011**, *7*, 5697.
- [6] S. Klaus, M. W. Lehenmeier, C. E. Anderson, B. Rieger, *Coord. Chem. Rev.* **2011**, *255*, 1460–1479.
- [7] G. Trott, P. K. Saini, C. K. Williams, *Philos. Trans. R. Soc. London Ser. A* **2016**, *374*, 20150085.
- [8] S. J. Poland, D. J. Darensbourg, *Green Chem.* **2017**, *19*, 4990–5011.
- [9] B. Grignard, S. Gennen, C. Jérôme, A. W. Kleij, C. Detrembleur, *Chem. Soc. Rev.* **2019**, *48*, 4466–4514.
- [10] Y. Wang, J. Fan, D. J. Darensbourg, *Angew. Chem. Int. Ed.* **2015**, *54*, 10206–10210; *Angew. Chem.* **2015**, *127*, 10344–10348.
- [11] J. Hilf, A. Phillips, H. Frey, *Polym. Chem.* **2014**, *5*, 814–818.
- [12] J. Langanke, A. Wolf, J. Hofmann, K. Böhm, M. A. Subhani, T. E. Müller, W. Leitner, C. Gürtler, *Green Chem.* **2014**, *16*, 1865–1870.
- [13] A. M. I. Stute, M. Meuresch, C. Gürtler, A. Wolf, R. Schomäcker, M. Gradzielski, M. Tupinamba Lima, V. J. Spiering (Covestro AG, Leverkusen, Germany), WO2019076862, **2018**.
- [14] D. J. Mitchell, G. J. T. Tiddy, L. Waring, T. Bostock, M. P. McDonald, *J. Chem. Soc. Faraday Trans. 1* **1983**, *79*, 975.
- [15] T. Kato, N. Taguchi, T. Terao, T. Seimiya, *Langmuir* **1995**, *11*, 4661–4664.
- [16] S. Radiman, C. Toprakcioglu, T. McLeish, *Langmuir* **1994**, *10*, 61–67.
- [17] G. T. Dimitrova, T. F. Tadros, P. F. Luckham, *Langmuir* **1995**, *11*, 1101–1111.
- [18] M. T. Lima, V. J. Spiering, S. N. Kurt-Zerdeli, D. C. Brüggemann, M. Gradzielski, R. Schomäcker, *Colloids Surf. A* **2019**, *569*, 156–163.
- [19] K. Shinoda, T. Yamaguchi, R. Hori, *Bull. Chem. Soc. Jpn.* **1961**, *34*, 237–241.
- [20] M. J. Rosen, A. W. Cohen, M. Dahanayake, X. Y. Hua, *J. Phys. Chem.* **1982**, *86*, 541–545.
- [21] A. W. Cohen, M. J. Rosen, *J. Am. Oil Chem. Soc.* **1981**, *58*, 1062–1066.
- [22] P. H. Elworthy, C. B. Macfarlane, *J. Pharm. Pharmacol.* **1962**, *14*, 100T–102T.
- [23] J. M. Corkill, J. F. Goodman, R. H. Ottewill, *Trans. Faraday Soc.* **1961**, *57*, 1627–1636.
- [24] S. Yada, T. Suzuki, S. Hashimoto, T. Yoshimura, *Langmuir* **2017**, *33*, 3794–3801.
- [25] M. J. Rosen, *Surfactants and Interfacial Phenomena*, Wiley, New York, **2004**.
- [26] P. Sakya, J. M. Seddon, R. H. Templer, R. J. Mirkin, G. J. T. Tiddy, *Langmuir* **1997**, *13*, 3706–3714.
- [27] H. Hoffmann, W. Ulbricht, *Curr. Opin. Colloid Interface Sci.* **1996**, *1*, 726–739.
- [28] M. Gradzielski, H. Hoffmann, G. Oetter, *Colloid Polym. Sci.* **1990**, *268*, 167–178.
- [29] K. L. Walther, M. Gradzielski, H. Hoffmann, A. Wokaun, G. Fleischer, *J. Colloid Interface Sci.* **1992**, *153*, 272–284.
- [30] K. Fontell, *Adv. Colloid Interface Sci.* **1992**, *41*, 127–147.
- [31] K. Mortensen, Y. Talmon, *Macromolecules* **1995**, *28*, 8829–8834.
- [32] N. F. Carnahan, K. E. Starling, *J. Chem. Phys.* **1969**, *51*, 635–636.
- [33] R. Kjellander, E. Florin, *J. Chem. Soc. Faraday Trans. 1* **1981**, *77*, 2053–2077.
- [34] P. G. Nilsson, B. Lindman, *J. Phys. Chem.* **1983**, *87*, 4756–4761.
- [35] J. Zhao, Z. N. Wang, X. L. Wei, F. Liu, W. Zhou, X. L. Tang, T. H. Wu, *Indian J. Chem. Sect. A* **2011**, *50*, 641–649.
- [36] B. von Szyszkowski, *Z. Phys. Chem.* **1908**, *64U*, 385–414.
- [37] E. Matijević, B. A. Pethica, *Trans. Faraday Soc.* **1958**, *54*, 587–592.
- [38] J. N. Phillips, *Trans. Faraday Soc.* **1955**, *51*, 561.
- [39] A. V. Feoktystov, H. Frielinghaus, Z. Di, S. Jaksch, V. Pipich, M.-S. Appavou, E. Babcock, R. Hanslik, R. Engels, G. Kemmerling, H. Kleines, A. Ioffe, D. Richter, T. Brückel, *J. Appl. Crystallogr.* **2015**, *48*, 61–70.
- [40] S.-H. Chen, T. L. Lin, *Methods Exp. Phys.* **1987**, *23B*, 489–543.

Manuscript received: October 16, 2019

Revised manuscript received: November 22, 2019

Accepted manuscript online: November 25, 2019

Version of record online: December 30, 2019